Traffic Performance Analysis of Handover in GMPCS Systems

Jaeweon Cho, *Student Member, IEEE,* and Daehyoung Hong, *Member, IEEE*

Abstract—This paper presents an analysis of handover process and its effect on the traffic performance in global mobile personal communications by satellite (GMPCS) systems. With the nongeostationary satellite used for the system, the handover scheme needs to be applied to make calls completed without any interruption. An analytical model is developed for the analysis of the handover process. We derive *mean number of handovers* and *handover delay* with various satellite antenna patterns and different settings of handover parameter. A suitable traffic model of the whole system is also derived after due considerations of the handover process. The system performance measures include *new call blocking probability, call dropping probability,* and *mean number of handovers per call.* A computer simulation is developed and used. We also analyze the system performance with a number of handover priority schemes applied. Based on the study results, handover parameters are selected to maximize the traffic performance. It is shown that we can improve overall traffic performance of GMPCS system by setting handover parameters properly and using the handover priority scheme.

Index Terms—Global mobile personal communications by satellite (GMPCS), handover, low earth orbit (LEO), mobile satellite communications, traffic performance.

I. INTRODUCTION

ONE of the main objectives of the next-generation mobile communication services is to provide communications between handheld personal terminals located at diverse locations around the world at any time. It does not seem possible to achieve this objective by means of only terrestrial mobile networks because of its limitation of service coverage. The global mobile personal communications by satellite (GMPCS) systems have been developed to provide the personal communication service anywhere at any time. A number of GMPCS systems are already operational for the commercial service.

GMPCS systems use a constellation of low or medium earth orbit (LEO or MEO) satellites. The nongeostationary satellites in LEO or MEO rotate the earth at very high speed. Whenever the satellite passes over the serving mobile terminal, a handover scheme needs to be applied to make calls completed without any interruption. Handovers occur from satellite to satellite, similar to the terrestrial cellular systems. However, unlike those cellular systems, the satellite beams move through mobile terminals rather than mobile terminals through the cells.

The authors are with the Department of Electronic Engineering, Sogang University, Seoul, 121-742, Republic of Korea (e-mail: jaeweon.cho@ieee.org; dhong@sogang.ac.kr).

Publisher Item Identifier S 0018-9545(01)09851-6.

The quality of service (QOS) of the whole system is affected by the handover process. If unnecessary handover occurs frequently in fringe of the satellite foot print, the signaling load can become too high. On the other hand, if the decision for handover is delayed too long, call can be dropped before handed over successfully. Such degradation of QOS can influence negatively on the system capacity. In order to provide high-quality services as well as to maximize the system capacity, we need to apply the handover process very carefully and optimally.

This paper analyzes the traffic performance of GMPCS systems with the handover process. Previous studies of GMPCS systems analyzed the traffic performance but without considering the handover process in real environment [1]–[4]. On the other hand, handover process and its effect on the traffic performance in terrestrial cellular systems were investigated in several papers. In this paper, the analytical handover model that Zhang and Holtzman [5] developed for terrestrial systems is extended to the case of GMPCS systems. The received signal strength model in GMPCS systems is developed and used for the analysis of the handover process. We also set a proper system level model and analyze the handover effect on QOS in GMPSC system. The channel characteristics affecting the handover process are also included in this paper for traffic performance analysis. In Section II, we analyze the handover process in a shadowed GMPCS environment. An analytical model is developed and used. A computer simulation is also developed to derive the handover effect on traffic performance. The performance results are shown in Section III. Finally, we draw conclusions in Section IV.

II. HANDOVER PERFORMANCE

A. Received Signal Level Model

The decision to initiate a handover can be made based on several quantities such as the received signal level from the connected satellite and neighbor satellites, and the distances from the satellites. At the coverage edge of a satellite, the elevation angle is low and the received signal level can be influenced by shadow fading. Since intersatellite handover occurs at the coverage edge, we cannot perform the handover process reliably based only on the distances. The received signal levels need to be measured and used for intersatellite handover process.

The received signal level model for the analysis of intersatellite handover is shown in Fig. 1. Since each satellite has a number of beams, intersatellite handover occurs between boundary beams. The signal level received from satellites 1 and 2 at time t, $r_1(t)$ and $r_2(t)$ (in dBW) are given by

$$r_1(t) = K_1 - K_2 \log d_1(t) + G_1(t) + \zeta_1(t) \quad (1)$$

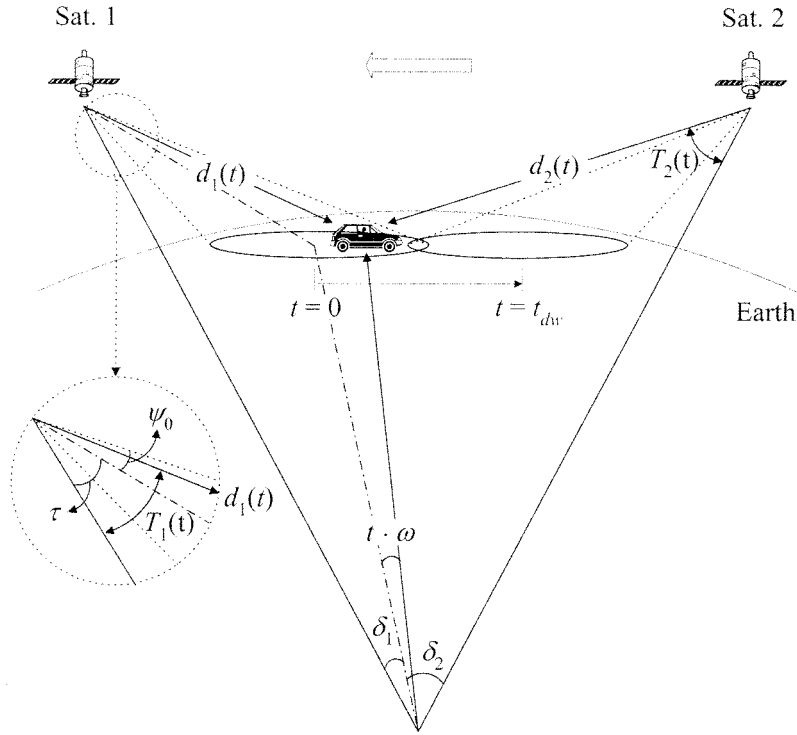$$r_2(t) = K_1 - K_2 \log d_2(t) + G_2(t) + \zeta_2(t) \quad (2)$$

Fig. 1.   The model of intersatellite handover.

where K_1 (in dBW) is the received signal level at a unit distance from satellite, and K_2 (in decibels per decade) is the slope of path loss (e.g., $K_2 = 20$ in free space). Satellites are moving in a fixed direction and their speed is much higher than that of mobiles. Therefore, the mobile's position can be represented by the distances from each satellite $d_1(t)$ and $d_2(t)$ (in kilometers) [6]. The distances are functions of time, and expressed as

$$d_1(t) = \sqrt{R_e^2 + R_o^2 - 2R_e R_o \cos(\delta_1 + t \cdot \omega)} \qquad (3)$$
$$d_2(t) = \sqrt{R_e^2 + R_o^2 - 2R_e R_o \cos(\delta_2 - t \cdot \omega)} \qquad (4)$$

where

R_e	radius of the earth (6378 km);
R_o	sum of orbit altitude and R_e;
ω	angular velocity of satellite (in degrees per second).

We assume in this work the reference mask for the radiation pattern of the satellite antenna as shown in Fig. 2 [7]. *Region a* corresponds to the part of main lobe that is out of coverage. In this region, the typical gain variation versus off-axis angle ψ is expressed as

$$G(\psi) = G_{\max} - 3(\psi/\psi_0)^s \qquad (5)$$

where $G_{\max}$ (in dBi) is the maximum antenna gain and ψ_0 (in degrees) is the half of the 3-dB beamwidth. The parameter s indicates the sharpness of the main lobe. From (5), the antenna gains of each satellite to the direction of mobile $G_1(t)$ and $G_2(t)$ (in dBi) are represented as

$$G_1(t) = G_{\max} - 3[(T_1(t) - \tau)/\psi_0]^s \qquad (6)$$
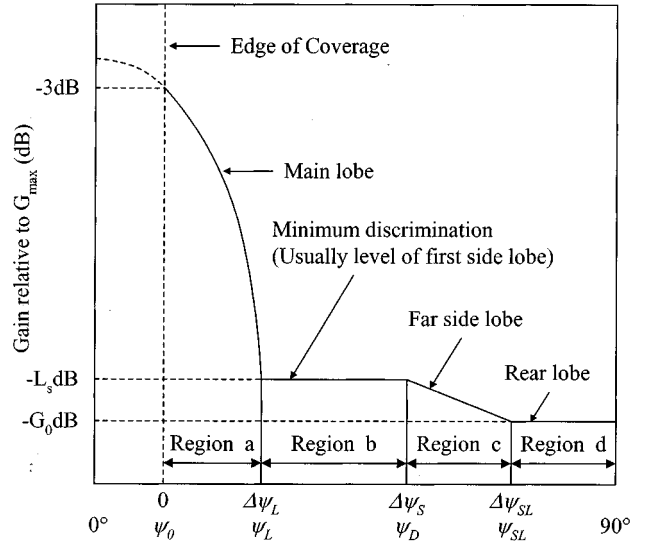$$G_2(t) = G_{\max} - 3[(T_2(t) - \tau)/\psi_0]^s \qquad (7)$$

Fig. 2.   Reference mask for antenna radiation pattern [7].

where

$$T_1(t) = \arcsin\left[\frac{R_e}{d_1(t)}\sin(\delta_1 + t \cdot \omega)\right] \qquad (8)$$

$$T_2(t) = \arcsin\left[\frac{R_e}{d_2(t)}\sin(\delta_2 - t \cdot \omega)\right] \qquad (9)$$

$$\tau = \arctan\left[\frac{\sin\delta_1}{R_o/R_e - \cos\delta_1}\right]. \qquad (10)$$

The detail derivation of these geometric parameters is given in Appendix I.

In (1) and (2), $\zeta_1(t)$ and $\zeta_2(t)$ (in decibels) are the shadow fadings of the signal level from each satellite. They are assumed

to be *Gaussian* processes and independent of each other. Mean $\mu_{\zeta_i}(t)$ and standard deviation $\sigma_{\zeta_i}(t)$ of the fading process depend on the satellite's elevation angle $\theta_i(t)$ as follows [8]:

$$\mu_{\zeta_i}(t) = \frac{20}{\ln 10} (-2.331 + 0.1142\theta_i(t) - 1.939$$
$$\times 10^{-3}\theta_i^2(t) + 1.094 \times 10^{-5}\theta_i^3(t)) \quad (11)$$
$$\sigma_{\zeta_i}(t) = 4.5 - 0.05\theta_i(t), \quad \text{for } 20° < \theta_i(t) < 80°. \quad (12)$$

Each shadowing process is also assumed to be correlated in time, and have an exponential correlation function like that in terrestrial cellular system environments [9]

$$E[\zeta_i(t)\zeta_i(t+\rho)] \approx \sigma_{\zeta_i}^2(t)\exp(-|\rho|/t_0) + \mu_{\zeta_i}^2(t). \quad (13)$$

In this equation, t_0 is defined as d_0/V_{mobile}, where d_0 is decor-relation distance and V_{mobile} is the mobile speed.

B. Mathematical Analysis

The performance of the handover process in terrestrial cellular systems is usually measured by *mean number of handovers and handover delay* [10]. The same parameters can also be used for handovers in GMPCS systems. When a mobile served by a satellite enters the service area of a new satellite, it is desirable that handover should be performed only once at the boundary of two service areas. One of the ways to prevent unnecessary handovers is to initiate the handover procedure based on the averaged signal levels. The measured signal levels at the mobile are averaged using window of duration T_w. Another way is to use a hysteresis margin h. Handover process is initiated if the averaged signal level of a new satellite exceeds that of the connected satellite by the hysteresis margin h. The difference between the averaged signal levels of two satellites will be expressed as

$$x(t) \equiv \bar{r}_1(t) - \bar{r}_2(t) = \frac{1}{T_w} \int_0^{T_w} r_1(t-\alpha) - r_2(t-\alpha) \, d\alpha. \quad (14)$$

We divide t_{dw} into N equal intervals for analysis, where t_{dw} is the period from the time when the center of the beam coverage of a satellite is located on the mobile to the time when that of the next satellite moves over the mobile. In this case, the sampling interval t_s is given by t_{dw}/N and the kth sampling point

t_k by kt_s. Let $P_{\text{ho}}(k)$ be the probability of one handover occurring in the kth interval, $P_{s2|s1}(k)$ the probability of handover from satellite 1 to satellite 2, and $P_{s1|s2}(k)$ the probability of handover from satellite 2 to satellite 1. Probabilities of a mobile being connected to each satellite, $P_{s1}(k)$ and $P_{s2}(k)$, can be recursively computed as follows [5]:

$$P_{\text{ho}}(k) = P_{s1}(k-1)P_{s2|s1}(k) + P_{s2}(k-1)P_{s1|s2}(k) \quad (15)$$
$$P_{s1}(k) = P_{s1}(k-1)[1 - P_{s2|s1}(k)] + P_{s2}(k-1)P_{s1|s2}(k) \quad (16)$$
$$P_{s2}(k) = P_{s2}(k-1)[1 - P_{s1|s2}(k)] + P_{s1}(k-1)P_{s2|s1}(k) \quad (17)$$

where $k = 1, 2, \ldots, N$, and $P_{s1}(0) = 1, P_{s2}(0) = 0$ as the initial values. Since $x(t_k)$ is a *Gaussian* process, $P_{s2|s1}(k)$ and $P_{s1|s2}(k)$ can be expressed in (18) and (19) shown at the bottom of the page, where $\mu_x(t_k)$ and $\sigma_x(t_k)$ denote the mean and the standard deviation of $x(k_k)$, respectively. If t_s is small, the satellite elevation angle does not change much during t_s. Hence, (18) and (19) are derived on the assumption that $\sigma_x(t_k)$ and $\sigma_x(t_{k-1})$ are identical. From (13) and (14), the covariance $C(t_k)$ of $x(t_k)$ and $x(t_{k-1})$, and $\sigma_x(t_k)$ are computed as follows (see Appendix II for detailed derivation):

$$C(t_k) = E[(x(t_k) - \mu_x(t_k))(x(t_{k-1}) - \mu_x(t_{k-1}))]$$
$$\approx \frac{2\sigma_{\zeta_i}^2(t_k)}{T_w^2} \left\{ t_0^2 \left[e^{(t_s-T_w)/t_0} + e^{-(t_s+T_w)/t_0} \right. \right.$$
$$\left. \left. - 2e^{-t_s/t_0} \right] + 2t_0(T_w - t_s) \right\} \quad (20)$$
$$\sigma_x^2(t_k) = E[(x(t_k) - \mu_x(t_k))^2]$$
$$\approx \frac{4\sigma_{\zeta_i}^2(t_k)}{T_w^2} \left[t_0^2(e^{-T_w/t_0} - 1) + t_0 T_w \right]. \quad (21)$$

Therefore, the correlation coefficient $\gamma(t_k)$ is given by (22) at the bottom of the page. $P_x(k_k)(\alpha)$ is the probability density function (pdf) for *Gaussian* random variable $x(k_k)$, and the Q function is defined as

$$Q(\beta) = \frac{1}{\sqrt{2\pi}} \int_\beta^\infty \exp(-y^2/2) \, dy. \quad (23)$$

$$P_{s1|s2}(k) \approx \Pr[x(t_k) > h \mid x(t_{k-1}) \leq h] \approx \frac{\int_h^\infty \left\{ 1 - Q \left[\frac{h - \mu_x(t_{k-1}) - \gamma(t_k)(\alpha - \mu_x(t_k))}{\sigma_x(t_{k-1})\sqrt{1-\gamma^2(t_k)}} \right] \right\} p_{x(t_k)}(\alpha) \, d\alpha}{1 - Q\left(\frac{h - \mu_x(t_{k-1})}{\sigma_x(t_k)}\right)} \quad (18)$$

$$P_{s2|s1}(k) \approx \Pr[x(t_k) < -h \mid x(t_{k-1}) \geq -h] \approx \frac{\int_{-\infty}^{-h} Q \left[\frac{-h - \mu_x(t_{k-1}) - \gamma(t_k)(\alpha - \mu_x(t_k))}{\sigma_x(t_{k-1})\sqrt{1-\gamma^2(t_k)}} \right] p_{x(t_k)}(\alpha) \, d\alpha}{Q\left(\frac{-h - \mu_x(t_{k-1})}{\sigma_x(t_k)}\right)} \quad (19)$$

$$\gamma(t_k) = \frac{C(t_k)}{\sigma_x(t_k)\sigma_x(t_{k-1})} \approx \frac{C(t_k)}{\sigma_x^2(t_k)} \approx \frac{t_0 \left[e^{(t_s-T_w)/t_0} + e^{-(t_s+T_w)/t_0} - 2e^{-t_s/t_0} \right] + 2(T_w - t_s)}{2t_0(e^{-T_w/t_0} - 1) + 2T_w}. \quad (22)$$

The number of handovers occurring during t_{dw} is equal to the number of intervals in which handovers occur. Therefore, the *mean number of handovers* can be defined as

$$\text{mean number of handovers} = \sum_{k=1}^{N} P_{\text{ho}}(k). \qquad (24)$$

Handover delay is defined as the period from the time when a mobile is located halfway between beams of two satellites to the time when handover is initiated. Therefore,

$$\text{handover delay} = k_{\text{cp}}t_s - t_{dw}/2 \qquad (25)$$

where the crossover point $k_{\text{cp}}t_s$ is defined as the time when $P_{s1}(k_{\text{cp}})$ is equal to 0.5.

C. Results

In order to analyze the handover performance using the proposed analytical method, we have selected Iridium as the system model. The system parameters are chosen from the case of the Iridium system such that orbit altitude is 780 km, angular velocity of satellite about 0.06°/s, number of satellites per orbital plane 11, and radius of the outer beam about 643.6 km [11]. Then the geometric parameters in Fig. 1 are computed as ψ_0 of 2.55°, δ_1 of 13.8°, δ_2 of 18.9°, and τ of 57.7°. If a mobile is located on the center of satellite 1's beam at 0 s, the mobile will be on the center of satellite 2's beam at 83.8 s. In this period, since the elevation angles of two satellites are below 20°, the standard deviation of shadowing is set to 3.5 dB by (12). Decorrelation distance of shadowing is assumed to be 20 m and the mobile speed to be 60 km/h.

Handover performance is influenced by the satellite antenna pattern. The width of the main lobe outside the 3-dB beamwidth is inversely proportional to the parameter s in (5). Hence, if s is decreased, the number of unnecessary handovers as well as handover delay can be increased because the region feasible for handover is extended. Fig. 3 shows the results at each setting of s. The *mean number of handovers* and *handover delay* are decreased as s is increased. It is found that handover performance can be improved by using the satellite antenna with the radiation pattern that goes down sharply out of the 3-dB beamwidth.

We evaluate the handover performance with varying handover parameters and show the results in Fig. 4. Fig. 4(a) shows that the *mean number of handovers* is decreased as the hysteresis margin or the period of the averaging window is increased. On the other hand, Fig. 4(b) shows that *handover delay* is increased as two handover parameters are increased. The results show that it is not easy to minimize both the *mean number of handovers* and *handover delay* at the same time.

The tradeoff of *handover delay* against the *mean number of handovers* is illustrated in Fig. 5. In the ideal case, the *mean number of handovers* will be one and *handover delay* 0 s. The region close to the ideal point is marked with a circle in the figure. It is desirable to decide the handover parameters around the region marked with a circle.

We have also developed a computer simulation to validate the analytical results. In the simulation, each performance measure
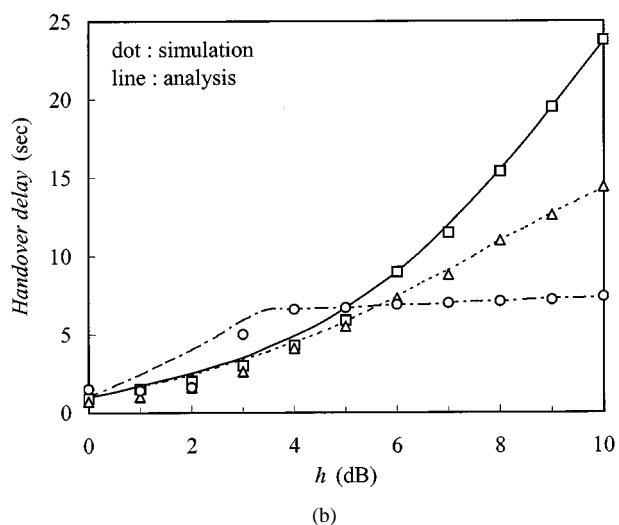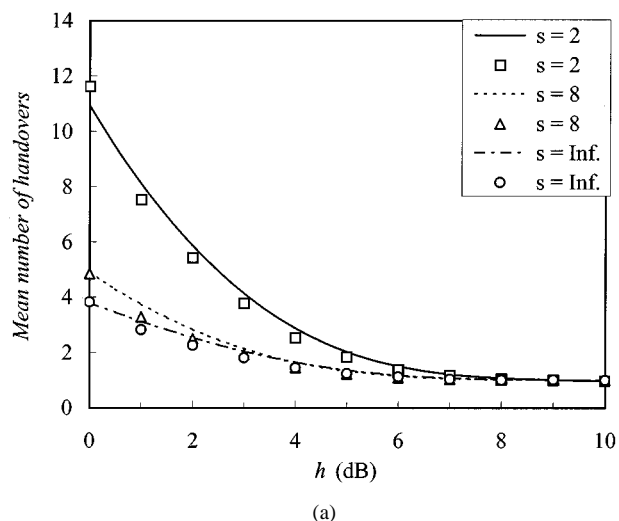

Fig. 3. Handover performance with various antenna patterns: $T_w = 2$ s. (a) Mean number of handovers. (b) Handover delay.

was obtained by using the *Monte Carlo* method, i.e., the shadowing sequence was generated with certain correlation in time. Simulation results are shown in the above figures. Almost all results of simulation and analytical method match well. It is confirmed by the simulation results that we can use the analytical method proposed and used in this section with confidence.

III. TRAFFIC PERFORMANCE WITH HANDOVER

A. Service Coverage Model

Satellites of GMPCS systems use the multibeam antenna in order to reduce the size of the mobile terminal, to increase the link capacity, and to improve the spectrum reuse efficiency. Fig. 6 shows the configuration of a multibeam antenna that is used for the traffic analysis. In order to simplify the simulation model, the multibeam antenna is modeled as shown in Fig. 6(b). It is assumed that the surface of earth is not spherical but flat and each antenna is located over the center of its foot print on the ground. Nevertheless, the received signal level at the mobile can be decided based on the real satellite distance and elevation angle, since both have been computed considering
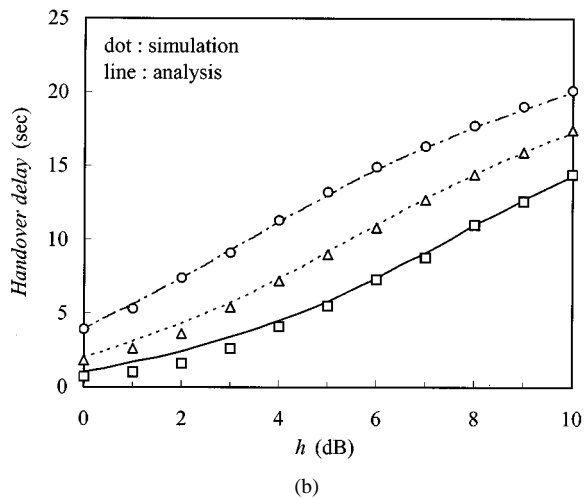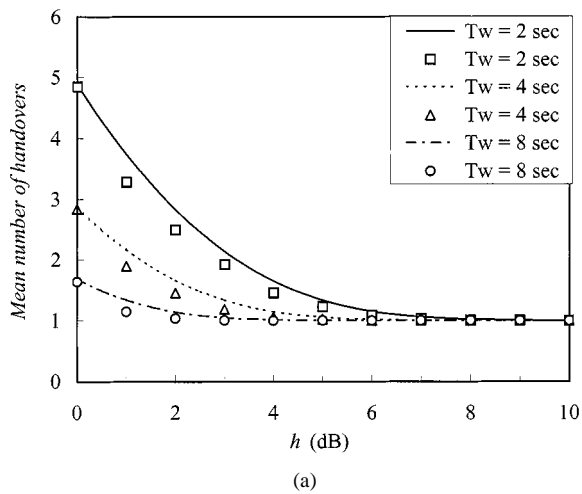
Fig. 4. Handover performance with varying handover parameters: $s = 8$. (a) Mean number of handovers. (b) Handover delay.
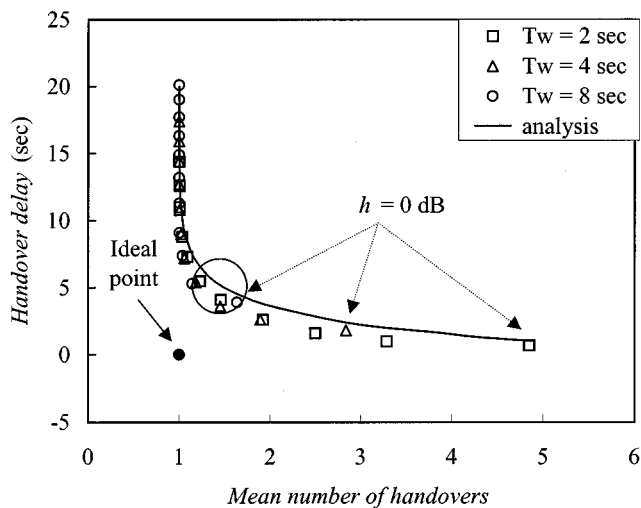

Fig. 5. A tradeoff curve of handover performance: $s = 8$.

the spherical surface. The proposed configuration model also makes the same 3-dB beamwidth applied to every antenna, so that all beam footprints on the ground can be identical.

If the multibeam antenna is designed so that the beam coverages on the ground are identical, the foot print of each beam will form a honeycomb pattern similar to the cell coverage of the terrestrial cellular systems [12]. The footprint can, therefore, be represented as shown in Fig. 7. Each satellite of Iridium is designed to have 48 beams [11]. In this figure, the thick solid line is the coverage boundary between adjacent satellites.

Because the multibeam footprint in Fig. 7 moves in the direction of satellite orbit, we can analyze the traffic performance of each polar orbit individually. Besides, the signal levels received from the satellite at the left and right side of the orbits can be symmetrical. Thus, each side can also be analyzed, respectively. We analyze the traffic performance of the left-side area that is marked with gray color in the figure.

B. System Parameters

The handover occurs frequently during a call duration because satellites pass over the mobile at very high speed. If no channel is immediately available in the target satellite beam, handover fails and the call can be forced to be terminated. The call drop due to handover failure can have much worse impact to user than the occurrence of a new call blocking. We must, therefore, apply the priority schemes to handover attempts. In this paper, we perform the analysis with two priority schemes, one with channels reserved for handovers and the other with queue for the handover [13]. The signal level received from satellite can vary rapidly due to shadowing. A call drop timer can be used to prevent an ongoing call from dropping due to short duration of signal level degradation.

The received signals from multiple beams of a satellite can be assumed to have identical shadowing. Hence, it is desirable that handover parameters such as hysteresis margin and averaging window may not be applied to intrasatellite handover process. We apply the following two handover initiation processes and compare their performances.

- *Type 1*: Handover parameters are applied to both inter and intrasatellite handover.
- *Type 2*: Handover parameters are applied to only intersatellite handover.

We have chosen the measures for the system performance as follows.

- *New call blocking probability*: The probability that a new call is blocked because there is no channel available or the received signal level is below the drop threshold.
- *Call dropping probability*: The probability that a call is forced to be terminated prematurely because the mobile experiences unsuccessful handover or received signal level is below the drop threshold until the call drop timer expires.
- *Mean number of handovers per call*: The mean number of handovers that the mobile experiences prior to completion or dropping of a call.

C. Simulation Results

A computer simulation has been developed and used to analyze the system traffic performance. Fig. 8 shows an orbital
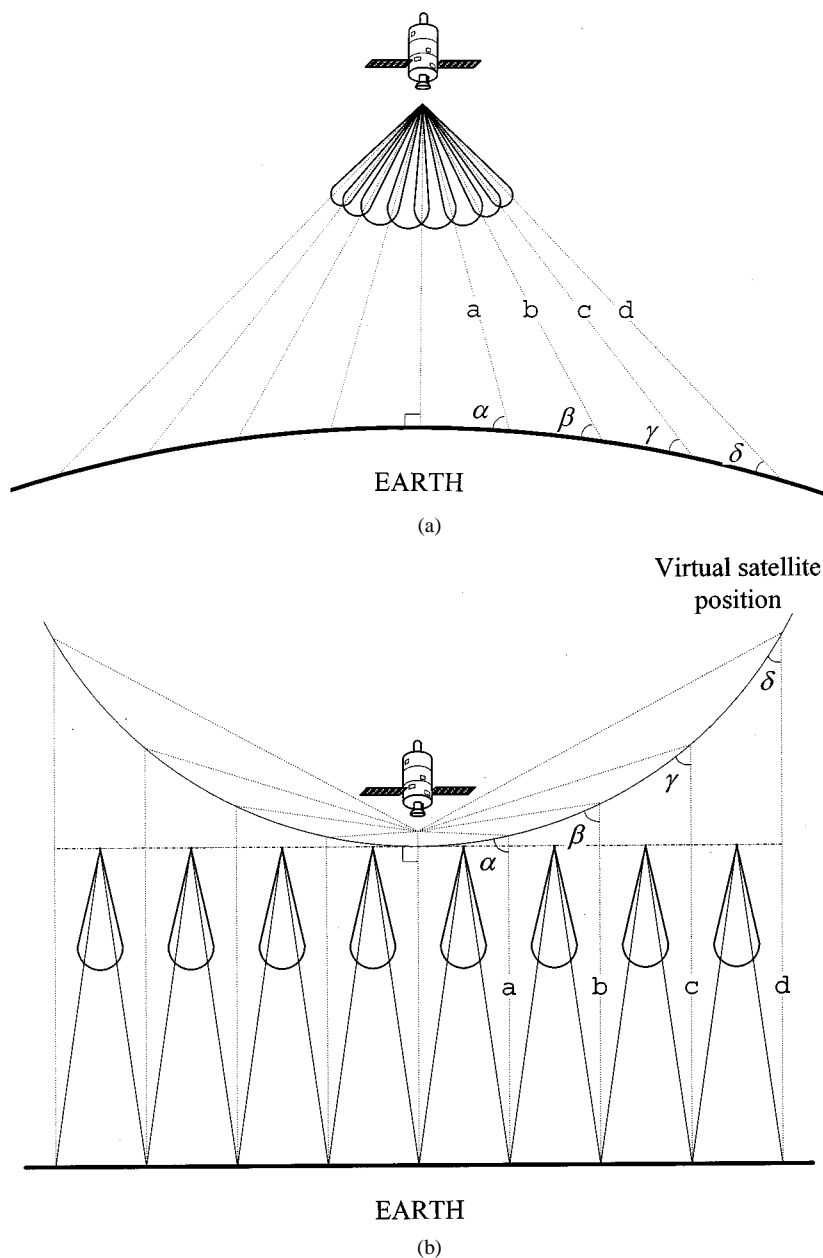
Fig. 6. Configuration of multibeam antenna. (a) Real configuration. (b) Virtual configuration.

plane chosen for the analysis. As described earlier, we have applied the analysis to the half side of the orbital plane (110°E–125°E and 40°W–55°W) as an example. We assume the following: calls are generated mostly and uniformly on the continents, traffic generated by each mobile is 0.02 erlang with the average call duration of 120 s, 10 channels are assigned to each beam, antenna gain $G_{\max}$ is 23 dBi [14], and the call drop timer is set to 2 s.

Even though a uniform traffic distribution has been assumed in this analysis, the simulation has been developed to adapt any form of traffic distributions. The shadowing process has been generated based on the elevation angle of the satellites.

The drop threshold T_{drop} (in dBW) is calculated as shown in (26). The link margin and the received signal level at the boundary of service coverage are considered. For example, the

Iridium system provides a mobile with the minimum satellite elevation angle of 8.2° and link margin of 16 dB [11]

$$
\begin{aligned}
T_{\mathrm{drop}} &= r_{\min} - \text{link margin} \\
&= K_1 - K_2 \log d_{\max} + G_{\max} - 3 - \text{link margin} \\
&= K_1 - 63.8 \tag{26}
\end{aligned}
$$

We divide the orbital plane into the unit area of 5° in latitude as well as in longitude, and then derive the traffic performance for every unit area. The results shown in Fig. 9 are for the case of 20 000 subscribers in the analyzed area (110°E–125°E and 40°W–55°W). Fig. 9(a) shows that more new calls are blocked at the inland area. It is because traffic demand is higher for the satellite passing over the inland area. As shown in Fig. 9(b),
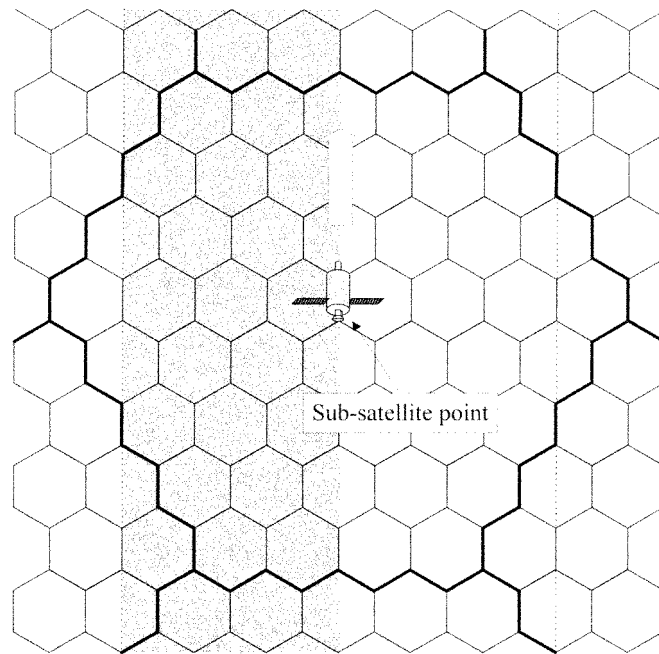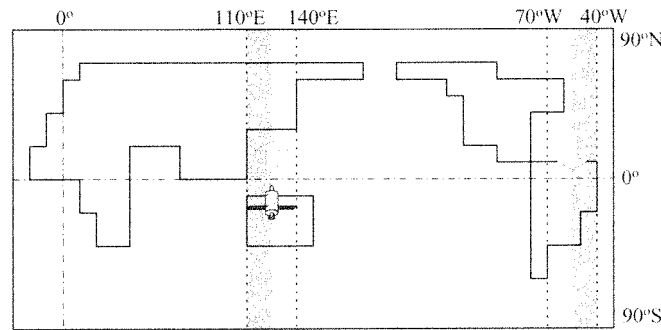
Fig. 7. Multibeam footprint on the ground.

Fig. 8. Orbital plane of Iridium.

call dropping probability is highest at the inland area close to the coverage boundary of the satellite due to the weak received signal level. The *mean number of handovers per call* is also highest at the coverage boundary of the satellite, where handovers can occur between satellites on different orbital planes, as shown in Fig. 9(c).

System performance has been analyzed with varying handover parameters and the results are shown in Fig. 10. In this figure, *call dropping probability* is plotted as functions of *mean number of handovers per call* with settings of $h = 0, 3, \ldots, 12$ (dB) and $T_w = 0, 2$ (s). The results are for the case of 18 000 subscribers in the analyzed area (110°E–125°E and 40°W–55°W). Every point illustrated in the figure represents the worst case of the unit areas in the analyzed region. The figure shows the tradeoff between *call dropping probability* and the *mean number of handovers per call*, and it is similar to that in Fig. 5. The result without shadowing is also plotted and marked as the ideal point in the figure. In this case, *call dropping probability* and the *mean number of handovers per call* can be minimized because handover occurs only once at the boundary between two beams. In the real environment

with shadowing, handover can occur more than once. The figure shows that the system performance can vary with setting of the handover parameters. Therefore, handover parameters need to be selected carefully in order to maximize the system performance.

In case of intrasatellite handover, the handover occurs only once at the boundary even though the handover parameters were not applied. If handover parameters were also applied to intrasatellite handover, it might introduce longer *handover delay*, which could cause a call drop. The figure shows that *Type 2* handover process can reduce both performance measures simultaneously to lower values than *Type 1*, as expected. The desirable operating point is the region close to the ideal point. Based on the results, we may select $h = 5$ dB and $T_w = 2$ s with *Type 2* handover process as a proper set of parameters. These parameter settings have been applied to the analysis described below.

Fig. 11 shows the traffic performance results with priority schemes for handover calls. In this figure, Ch_HO denotes the number of channels reserved only for handover. The figure shows that *call dropping probability* is decreased but *new call blocking probability* is increased as Ch_HO is increased. As an
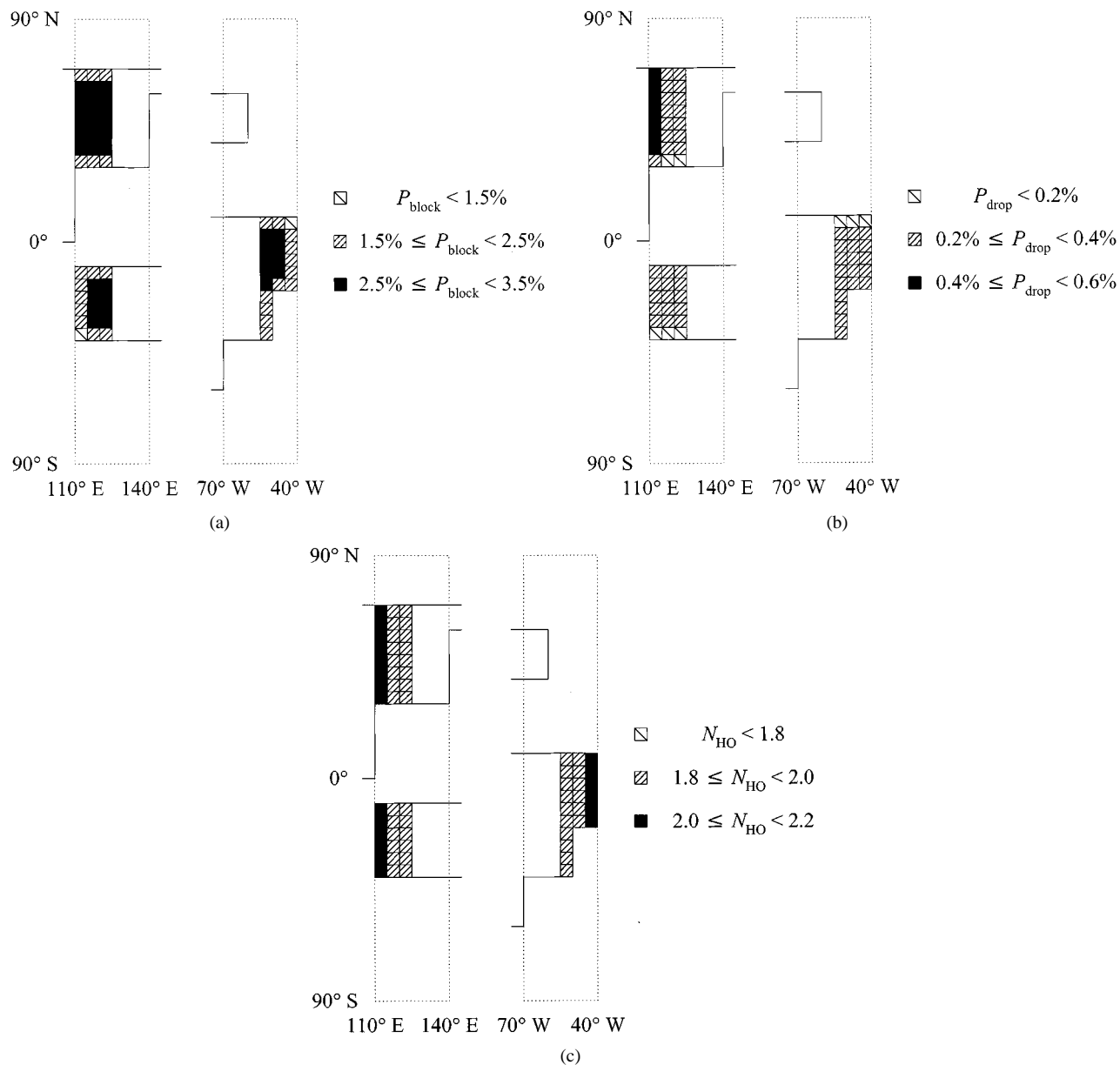
(a)

(b)

(c)

Fig. 9. Performance results from each unit area: number of subscribers $= 20\,000$, Type 1 handover process $h = 4$ dB, $T_w = 2$ s, handover queue is used, number of channels for handovers $= 0$. (a) New call blocking probability. (b) Call dropping probability. (c) Mean number of handovers per call.
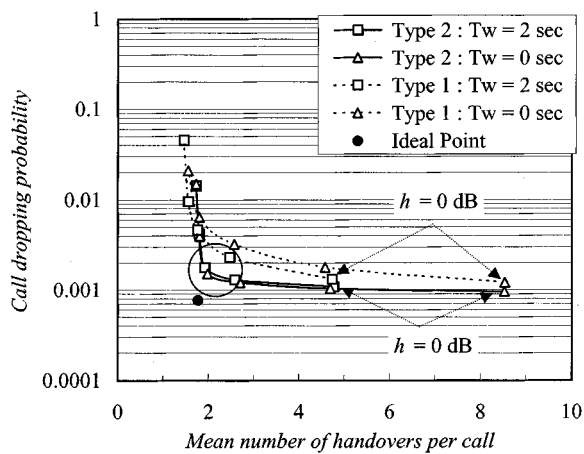

Fig. 10. Tradeoff curve of traffic performance: number of subscribers $= 18\,000$, handover queue is used, number of channels for handovers $= 0$.
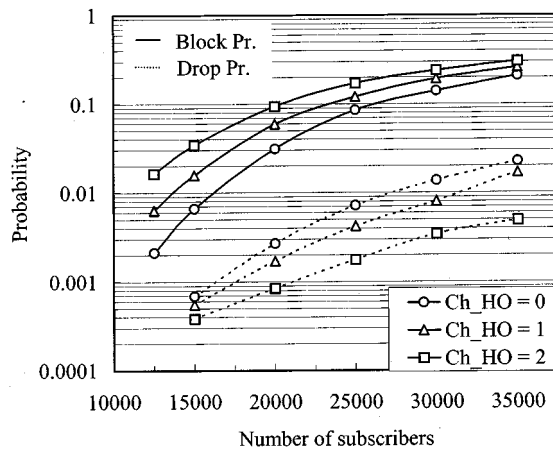

Fig. 11. The performance of handover priority scheme: Type 2 handover process $h = 5$ dB, $T_w = 2$ s, handover queue is used.

example, we have analyzed the system which has the required QOS of *new call blocking probability* below 2% and *call dropping probability* below 0.1%. With this QOS goals, subscribers for the system can be maximum at 16 000 when one channel or no channel is reserved for handover calls.

IV. CONCLUSION

An analytical model has been developed and used to analyze the handover process of the GMPCS system. The *mean number of handovers* and *handover delay* have been derived for various satellite antenna patterns and different settings of handover parameters. Both performance measures are decreased with sharper antenna radiation pattern out of 3-dB beamwidth. On the other hand, it is not easy to minimize both the *mean number of handovers* and *handover delay* at the same time by controlling the handover parameters such as averaging window duration and hysteresis margin. Nevertheless, the handover parameters can be selected properly from the tradeoff between those performance measures.

A simulation model has been developed and used to analyze the overall traffic performance of the GMPCS system with handover process. The system performance in each region depends on the traffic load and the received signal strength. The system performance measures, *call dropping probability* and the *mean number of handovers per call*, are also influenced by the setting of the handover parameters. Results show that there is a tradeoff between those performance measures. A number of handover priority schemes can also be applied to increase the system capacity. It is shown that the overall traffic performance of the GMPCS system can be improved by setting system parameters properly and using the handover priority scheme.

The models and analysis results presented in this paper can be utilized for setting the handover parameters to maximize the traffic performance of GMPCS systems. This study can be extended to the analysis of the effect of various handover algorithms as in [15]. The developed simulation models are flexible, and can be applied to further studies such as dynamic resource management techniques for GMPCS systems.

APPENDIX I
REPRESENTATION OF GEOMETRIC PARAMETERS

The tilt angle T_x is to be represented as the function of the central angle δ_x. T_x is measured at the satellite from the sub-satellite point to the ground station, as shown in Fig. 12.

From the triangle in the figure, we obtain, using the law of sines

$$\frac{\sin T_x}{R_e} = \frac{\sin \delta_x}{d_x} = \frac{\sin(90° + \theta_x)}{R_o}. \tag{27}$$

Therefore, T_x is given by

$$T_x = \arcsin\left(\frac{R_e}{d_x}\sin\delta_x\right). \tag{28}$$

Substituting T_x by $T_1(t)$, d_x by $d_1(t)$, and δ_x by $\delta_1 + t \cdot \omega$, we get (8). Equation (9) is obtained in a similar manner by substituting
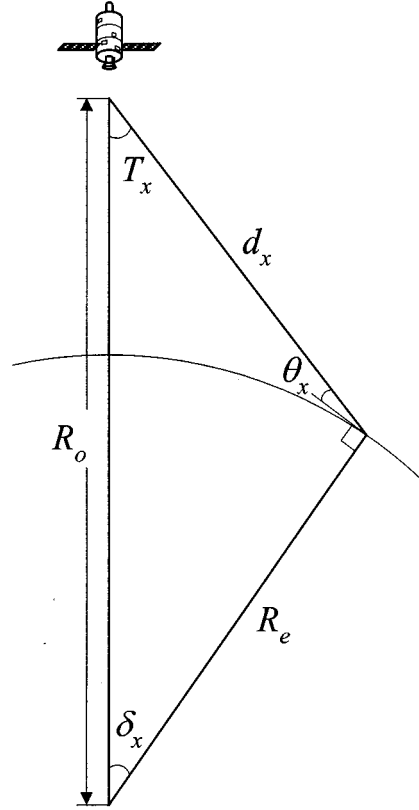

Fig. 12. Simple satellite geometry.

T_x by $T_2(t)$, d_x by $d_2(t)$, and δ_x by $\delta_2 - t \cdot \omega$. We can also rewrite (27) as

$$\sin T_x = \frac{R_e}{R_o}\sin(90° + \theta_x)$$
$$= \frac{R_e}{R_o}\sin(T_x + \delta_x)$$
$$= \frac{R_e}{R_o}(\sin T_x \cos \delta_x + \cos T_x \sin \delta_x). \tag{29}$$

Note from Fig. 12 that $T_x + \delta_x + \theta_x = 90°$. Dividing both sides by $\cos T_x$ and solving for T_x, we obtain

$$T_x = \arctan\left(\frac{\sin \delta_x}{R_o/R_e - \cos \delta_x}\right). \tag{30}$$

Substituting T_x by τ and δ_x by δ_1, we get (10).

APPENDIX II
EVALUATION OF COVARIANCE

Covariance $C(t_k)$ of $x(t_k)$ and $x(t_{k-1})$ is to be derived. We begin by rewriting the shadowing process $\zeta_i(t)$ as *Gaussian* process $\xi_i(t)$ with zero mean

$$\zeta_i(t) = \xi_i(t) + \mu_{\zeta_i}(t), \qquad \text{for } i = 1 \text{ and } 2. \tag{31}$$

This analysis focuses on the intersatellite handover on a polar orbital plane. The mobile that locates in fringe of a satellite foot print, views surrounding satellites at almost the same elevation angles. Therefore, we can assume the variances of both random

processes in (31) to be the same. In order to simplify the derivation, they are assumed to be constant as

$$\text{Var}[\xi_1(t)] = \sigma_{\zeta_1}^2(t) \approx \sigma_{\zeta_2}^2(t) \approx \sigma_\xi^2. \tag{32}$$

The means of $\zeta_1(t)$ and $\zeta_2(t)$ can also be assumed to be the same. Therefore

$$\begin{aligned}
\mu_x(t) &\equiv E[x(t)] \\
&= \frac{1}{T_w} \int_0^{T_w} E[r_1(t-\alpha) - r_2(t-\alpha)] \, d\alpha \\
&= \frac{1}{T_w} \int_0^{T_w} \left(K_2 \log \frac{d_2(t-\alpha)}{d_1(t-\alpha)} \right. \\
&\quad \left. + G_1(t-\alpha) - G_2(t-\alpha) \right) d\alpha.
\end{aligned} \tag{33}$$

Using the definition of covariance and referring to (13), (14), and (33), we derive

$$\begin{aligned}
C(t_k) &\equiv E[(x(t_k) - \mu_x(t_k))(x(t_{k-1}) - \mu_x(t_{k-1}))] \\
&= \frac{1}{T_w^2} \int_0^{T_w} \int_0^{T_w} E[(\xi_1(t_k - \alpha_1) - \xi_2(t_k - \alpha_1)) \\
&\quad \times (\xi_1(t_k - t_s - \alpha_2) - \xi_2(t_k - t_s - \alpha_2))] \, d\alpha_1 \, d\alpha_2 \\
&\approx \frac{2\sigma_\xi^2}{T_w^2} \int_0^{T_w} \int_0^{T_w} e^{-|\alpha_1 - t_s - \alpha_2|/t_0} \, d\alpha_1 \, d\alpha_2 \\
&\approx \frac{2\sigma_{\zeta_i}^2(t_k)}{T_w^2} \left\{ t_0^2 \left[e^{(t_s - T_w)/t_0} + e^{-(t_s + T_w)/t_0} \right. \right. \\
&\quad \left. \left. - 2e^{-t_s/t_0} \right] + 2t_0(T_w - t_s) \right\}.
\end{aligned} \tag{34}$$

From (34), the variance $\sigma_x^2(t_k)$ can be derived as

$$\begin{aligned}
\sigma_x^2(t_k) &\equiv E[(x(t_k) - \mu_x(t_k))^2] = C(t_k)|_{t_s=0} \\
&\approx \frac{4\sigma_{\zeta_i}^2(t_k)}{T_w^2} \left[t_0^2(e^{-T_w/t_0} - 1) + t_0 T_w \right].
\end{aligned} \tag{35}$$

REFERENCES

[1] F. Dosiere and G. Maral, "Handover model and applications to LEO systems dimensioning," in *Proc. AIAA 15th Int. Communications Satellite System Conf.*, San Diego, CA, Mar. 1994, pp. 770–774.

[2] E. D. Re, R. Fantacci, and G. Giambene, "Efficient dynamic channel allocation techniques with handover queueing mobile satellite networks," *IEEE J. Select. Areas Commun.*, vol. 13, pp. 397–405, Feb. 1995.

[3] A. Ganz, B. Li, and Y. Gong, "Performance study of low earth-orbit satellite systems," *Proc. IEEE Int. Conf. Communications (ICC)*, pp. 1098–1102, May 1993.

[4] P. Carter and M. A. Beach, "Evaluation of handover mechanisms in shadowed low earth orbit land mobile satellite systems," *Int. J. Satellite Commun.*, vol. 13, no. 3, pp. 177–190, May–June 1995.

[5] N. Zhang and J. M. Holtzman, "Analysis of handoff algorithms using both absolute and relative measurements," *IEEE Trans. Veh. Technol.*, vol. 45, pp. 174–179, Feb. 1996.

[6] W. L. Pritchard, H. G. Suyderhoud, and R. A. Nelson, *Satellite Communication Systems Engineering.* Englewood Cliffs, NJ: Prentice-Hall, 1993.

[7] *Satellite Antenna Radiation Pattern for Use as a Design Objective in Fixed-Satellite Service Employing Geostationary Satellites*, Std. ITU-R Rec. S. 672, 1995. Int. Telecomm. Union, Geneva, Switzerland.

[8] G. E. Corazza and F. Vatalaro, "A statistical model for land mobile satellite channels and its application to nongeostationary orbit systems," *IEEE Trans. Veh. Technol.*, vol. 43, pp. 738–742, Aug. 1994.

[9] P. Taaghol and R. Tafazolli, "Correlation model for shadow fading in land-mobile satellite systems," *Electron. Lett.*, vol. 33, no. 15, pp. 1287–1289, July 1997.

[10] R. Vijayan and J. M. Holtzman, "A model for analysis handoff algorithms," *IEEE Trans. Veh. Technol.*, vol. 42, pp. 351–356, Aug. 1993.

[11] R. J. Leopold, "Low-earth orbiting satellite system," in *Proc. ICUPC'92 Workshop on Personal Communication Systems*, Dallas, TX, Oct. 1992, pp. 69–92.

[12] M. A. Pullman, K. M. Peterson, and Y. Jan, "Meeting the challenge of applying cellular concepts to LEO satcom systems," *Proc. IEEE Int. Conf. Communications (ICC)*, pp. 770–773, June 1992.

[13] D. Hong and S. S. Rappaport, "Traffic model and performance analysis for cellular mobile radio telephone systems with prioritized and non-prioritized handoff procedures," *IEEE Trans. Veh. Technol.*, vol. 35, pp. 77–92, Aug. 1986.

[14] K. G. Johannesen and S. K. Park, "LEO, MEO and GEO mobile satellite performance comparison," in *Proc. Int. Conf. Telecommunication (ICT)*, Nusa Dua, Indonesia, Aug. 1995, pp. 138–142.

[15] W. R. Mende, "Evaluation of a proposed handover algorithm for the GSM cellular system," in *Proc. 40th IEEE Vehicular Technology Conf. (VTC)*, Orlando, FL, May 1990, pp. 264–269.

Jaeweon Cho (S'95) received the B.S. and M.S. degrees in electronic engineering from Sogang University, Korea, in 1995 and 1997, respectively. He is currently working toward the Ph.D. degree at the Department of Electronic Engineering, Sogang University.

From 1997 to 1998, he was with the R&D Center of DACOM, Korea, where he engaged in the research on IMT-2000 systems. Since 1998, he has been a Research Assistant at Sogang University, Korea. His research interests include radio resource management and mobility management for mobile communication systems and global mobile personal communications by satellite (GMPCS) systems.

Daehyoung Hong (S'76–M'86) received the B.S. degree in electronics engineering from the Seoul National University, Seoul, Korea, in 1977, and the M.S. and Ph.D. degrees in electrical engineering from the State University of New York at Stony Brook, in 1982 and 1986, respectively.

He was a Faculty Member of the Electrical and Electronics Engineering Department of ROK Air Force Academy and an air force officer from 1977 to 1981. He joined Motorola Communication Systems Research Laboratories in 1986 where he was a Senior Staff Research Engineer and participated in the research and development of digital trunked radio systems (TRS) as well as CDMA digital cellular systems. He joined the faculty of the Electronic Engineering Department of Sogang University, Seoul, Korea, in 1992, where he is currently Professor and Chair. During the academic year 1998–1999, he was a Visiting Associate Professor at the University of California, San Diego, working in the Center for Wireless Communications. His research interests include design, performance analysis, control algorithms, and operations of wireless access network and communication systems. He has published numerous technical papers and holds several patents in the areas of wireless communication systems. He has been a Consultant for a number of industrial firms. He served as a Division Editor for Wireless Communications of the *Journal of Communications and Networks*.

Dr. Hong is a member of the Korea Institute of Communication Sciences (KICS) and the Institute of Electronic Engineers Korea (IEEK). He has been active in a number of professional societies. His service includes: Chairman, Korea Chapter, IEEE Communications Society; Chairman, Mobile Communications Technical Activity Group, KICS; Chairman, Communications Society, IEEK; and Technical Program Committees for several major conferences. He is now Chair of Meeting & Conference Committee at the Asia Pacific Region of the IEEE ComSoc and also Chair of the Technical Program Committee for CDMA International Conference this year (CIC2001). He is also a member of Tau Beta Pi and Eta Kappa Nu.